# 学位論文

**A procedure for method development and protein binding ratio as the indicator of sensitivity with anticancer agents on MALDI mass spectrometry imaging**
**（抗がん剤を用いた MALDI-質量分析イメージングの測定メソッド開発手順と感度の指標としてのタンパク結合率）**

林　善治

Yoshiharu　Hayashi

熊本大学大学院医学教育部博士課程医学専攻
腫瘍治療・トランスレーショナルリサーチ学

指導教員

濱田　哲暢　客員教授

熊本大学大学院医学教育部博士課程医学専攻
腫瘍治療・トランスレーショナルリサーチ学

2023 年 3 月

# 学　位　論　文

論文題名　：　**A procedure for method development and protein binding ratio as the indicator of sensitivity with anticancer agents on MALDI mass spectrometry imaging**
（抗がん剤を用いた MALDI-質量分析イメージングの測定メソッド開発手順と感度の指標としてのタンパク結合率）

著 者 名　：　林　善治
Yoshiharu　Hayashi

指導教員名　：　熊本大学大学院医学教育部博士課程医学専攻
腫瘍治療・トランスレーショナルリサーチ学
濱　田　哲　暢　客員教授

審査委員名　：　臨床病態解析学担当教授　松　井　啓　隆
資源開発学担当教授　竹　尾　透
腫瘍医学担当准教授　荒　木　令　江
消化器外科学担当特任准教授　石　本　崇　胤

2023年3月

Drug Metabolism and Pharmacokinetics 38 (2021) 100385

Contents lists available at ScienceDirect

Drug Metabolism and Pharmacokinetics

journal homepage: http://www.journals.elsevier.com/drug-metabolism-and-pharmacokinetics

Regular Article

# A procedure for method development and protein binding ratio as the indicator of sensitivity with anticancer agents on MALDI mass spectrometry imaging

Yoshiharu Hayashi [a, b, c], Mayu Ohuchi [a, b], Shoraku Ryu [a], Shigehiro Yagishita [a], Akinobu Hamada [a, b, *]

[a] Division of Molecular Pharmacology, National Cancer Center Research Institute, 5-1-1 Tsukiji, Chuo-ku, Tokyo, 104-0045, Japan
[b] Department of Medical Oncology and Translational Research, Graduate School of Medical and Pharmaceutical Sciences, Kumamoto University, 1-1-1 Honjo, Chuo-ku, Kumamoto, 860-8556, Japan
[c] Bioanalysis Research Department, CMIC Pharma Science Co., Ltd., 17-18 Nakahata-cho,Nishiwaki, Hyogo, 677-0032, Japan

ARTICLE INFO

*Article history:*
Received 2 July 2020
Received in revised form
21 December 2020
Accepted 20 January 2021
Available online 30 January 2021

*Keywords:*
MALDI-MS
Pharamaco-imaging
Protein binding ratio
Hydrophilicity
Hydrophobicity

ABSTRACT

The concentration and distribution of a drug and its metabolites in tissues are key factors for elucidating both drug efficacy and toxicity in drug development. In this study we developed a pharamaco-imaging procedure for 12 agents and investigated the relationship between the properties of target compounds and the sensitivities of detection in matrix-assisted laser desorption/ionization-mass spectrometer imaging (MALDI-MSI). We prepared mock samples with mouse liver homogenates diluted with gelatin solution, limit of detection concentrations of each compound was confirmed. The correlation was evaluated between the intensities of mass signals obtained in MALDI-MSI with each test compound (the intensities of the test compounds) at a consistent concentration and the properties of each test compound. The liver homogenate diluted with gelatin solution showed easier handling and lower coefficients of variation than did liver homogenate only, and can be used as a good surrogate matrix. Based on the analysis of 12 agents, the protein binding ratios showed significant correlation to the detection sensitivities. We presented a procedure for standardization of pharmaco-imaging method development with an in-tissue method using MALDI-MS. Our results indicated the correlation between test compound's sensitivity and their protein binding ratios in plasma or serum.



## 1. Introduction

In drug development, drug delivery to target sites is one of the most crucial issues since this property directly relates to drug efficacy. Therefore, it is essential to develop appropriate assay methods that can evaluate the concentrations of drugs at target sites. The liquid chromatography-mass spectrometry (LC/MS) is highly sensitive and selective and now considered one of the standard tools for drug development. However, the major disadvantage of the LC/MS is that the information on the spatial distribution of the administered drug and its metabolites in tissues are lost in the process of the extraction of target compounds and their metabolites from collected samples [1,2].

Alternatively, imaging technologies provide methods that compensate for the above disadvantage. Imaging with autoradiography (ARG) often has been used classically in pharmacokinetic studies[3]. ARG, however, also has problems such as the indispensable requirement for a radioisotope-labeled compound (RI), and it can be difficult to distinguish the administered compound from its metabolites. Recently, imaging with matrix-assisted laser desorption/ionization-mass spectrometry (MALDI-MS) is becoming increasingly prominent in pharmacokinetic studies as a technique that resolves those issues [4–11].

The concept of MALDI-MSI was introduced in 1997 by Caprioli et al. for the rapid and direct profiling of the analytes within a tissue section or an organ [12,13]. In this process, first, the matrix is uniformly deposited over various tissue sections to produce mixed crystals with components containing the tissue sections. Second,

* Corresponding author. Department of Pharmacology and Therapeutics, Fundamental Innovative Oncology Core, National Cancer Center Research Institute, Tsukiji 5-1-1, Chuo-ku, Tokyo, 104-0045, Japan.
*E-mail address:* akhamad@ncc.go.jp (A. Hamada).

https://doi.org/10.1016/j.dmpk.2021.100385

pulsed laser irradiation of the sample over a predetermined two-dimensional array directly generates ion plumes. Third, the analyte molecules are ionized by being protonated or deprotonated in the hot plume of ablated gases. Fourth, the ionized molecules are introduced into a MS for analysis [14,15].

For bioanalytical method development using MS, the conditions of pretreatment and ionization are crucial parameters. When samples are analyzed by LC/MS, the test compounds are extracted from collected samples (pretreatment), and subsequently analyzed (ionized) after separation on a column. Therefore, we often investigate the optimized conditions of extraction and ionization separately. (A biological sample is used to optimize the extraction condition, and pure test compound [not include biological component] is used to optimize the operating parameters.) The ease of ionization of target compounds is empirically estimated using target compounds' properties, such as pKa, Log P, and polarizability. In the case of MALDI-MSI, extraction and ionization are almost simultaneously carried out in the same spot. Thus, a (mimetic) sample is required that both extraction and ionization can be optimized. Suitable mimetic samples must be homogeneous and easy to obtain, and must closely match the properties of the analyte present in the actual samples. Four principal approaches for quantification via MALDI-MSI have been reported: the in-solution method, the on-tissue method, the in-tissue method, and the serial section method[16]. Preparation of the mimetic samples by the in-tissue method is favored, because the in-tissue method analyzes mimetic samples prepared by spiking test compounds in the blank tissue homogenate, thereby reflecting most of the properties of the analyte present in the real sample. In the present work, we focused on target compounds in the tissues; the majority of such target compounds are bound to proteins in the tissues. Like pKa, Log P, and polarizability, the protein binding ratio is expected to be a key parameter for the development of assay methods incorporating MALDI-MSI.

We here presented a procedure for standardization of pharmaco-imaging method development using the in-tissue method with MALDI-MS against 12 agents [10 anticancer agents (afatinib, dasatinib, docetaxel, erlotinib, fluorouracil, gefitinib, imatinib, nilotinib, olaparib, and osimertinib), 1 antiviral agent (raltegravir), and 1 hypoglycemic agent (sitagliptin)]. Moreover, we estimated key parameters affecting the intensities of the target compounds by investigating the relationship between the sensitivities of target compounds and those properties.

## 2. Materials and methods

### 2.1. Reagents and materials

Afatinib, osimertinib, and gefitinib were purchased from Chemscene (Monmouth Junction, NJ, USA). Dasatinib, erlotinib, imatinib, olaparib, and nilotinib were purchased from Selleck Chemicals (Houston, TX, USA). Fluorouracil was purchased from Tokyo Chemical Industry (Tokyo, Japan). Raltegravir was purchased from Toronto Research Chemicals (North York, ON, Canada). Sitagliptin (sitagliptin phosphate), α-cyano-4-hydroxycinnamic acid (α-CHCA), 2,5-dihydroxybenzoic acid (DHB), and gelatin from porcine skin were purchased from Sigma-Aldrich (St. Louis, MO, USA). HPLC-grade trifluoroacetic acid (TFA), and LC-MS-grade methanol were purchased from Kanto Chemical Co. (Tokyo, Japan). Docetaxel, formic acid (FA), LC-MS-grade acetonitrile, and acetone were purchased from Wako Pure Chemical Industries (Osaka, Japan). Blank tissue (mouse liver tissue was used herein as example) was collected in National Cancer Center Research Institute. That was approved by the Institutional Animal Ethics Committee of the National Cancer Center Research Institute (Permission Number: T17-073-M02) and carried out in accordance with the guidelines.

### 2.2. Preparation of sample blocks

Each test compound was dissolved in 50% methanol solution to prepare a standard solution. A portion of mouse liver was transferred to a 0.5-mL polypropylene tube to prepare a homogenate [17]. As a first step, the liver was homogenized with zirconium beads (ZB-10; TOMY SEIKO, Tokyo, Japan) for 120 s at 5000 rpm using a TOMY Microsmash™ MS-100R (TOMY SEIKO). Next, a portion of the liver homogenate was transferred to a 2.0-mL polypropylene tube and weighed; the homogenate then was mixed with an equal weight of a 100-mg/mL gelatin solution to yield a 50% homogenate. Aliquots of the 50% homogenate were dispensed into other 2.0-mL polypropylene tubes and spiked with one of the standard solutions; the resulting mixtures were shaken on a vortex mixer, yielding homogenates containing the test compounds at final concentrations of 10 ng/mg (10 ng/mg in the 50% homogenate is equivalent to 20 ng/mg in pure liver; hereafter, concentrations are described as concentrations in liver homogenate).

To prepare (the limit of detection) LOD test samples, the homogenates at 20 ng/mg were prepared by serial dilution in blank homogenate using pipettes. The concentrations (ng/mg) of each test compound were as follows: afatinib: 1, 0.5, 0.25, and 0.1; dasatinib: 2, 1, 0.5, 0.25, 0.1, and 0.05; erlotinib: 0.1, 0.05, 0.025, and 0.01; gefitinib: 1, 0.5, 0.25, and 0.1; nilotinib: 4, 2, 1, 0.5, 0.2, 0.1, and 0.05; imatinib: 20, 10, 5, 2, 1, 0.5, and 0.2; osimertinib: 20, 10, 5, and 2.5; olaparib: 20, 10, 5, 2, and 1; raltegravir: 10, 5, 2.5, 1, and 0.5; and sitagliptin: 10, 5, 2, and 1.

A solution of gelatin at 100 mg/mL was poured into a mold (Tissue-Tek Cryomold No. 4566; Sakura Finetek, Torrance, USA) and allowed to cool at 4 °C for 30 min. A spuit (polyethylene spoids 1-4656-01, As One Corporation, Osaka, Japan) was used to generate holes in the surface of the solidified gelatin. The homogenate samples were injected carefully into the holes in the gelatin and the block then was rapidly frozen with dry ice.

The prepared gelatin block was sliced into 8-μm sections at −20 °C using a cryo-microtome (CM1950; Leica Microsystems K·K., Tokyo, Japan) [7,10]. The obtained sections were mounted on an indium tin oxide-coated glass slide (Matsunami Glass, Osaka, Japan), and ionization agents (matrices) then were deposited onto the sections [7,10].

### 2.3. Matrix deposition

α-CHCA and DHB were selected as ionization agents (referred to as "matrices") [11,15,18]. A solution of α-CHCA at 7 mg/mL was prepared in 0.1% TFA or FA containing 50% acetone; a solution of DHB at 30 mg/mL was prepared in 0.1% TFA or FA containing 50% acetonitrile. These matrix solutions were sprayed by using an ultrafine sprayer system (SMALDIprep, TransMIT, Giessen, Germany) or a hand sprayer (GSI Creos, Tokyo, Japan) [7,10]. A description of the matrix deposition conditions employed here is provided in Electronic Supplementary Material (ESM), Tabs. S1 and S2.

### 2.4. Reference sample

Reference samples were prepared to investigate the intensities of pure test compounds (without biological components). The reference sample was prepared by mixing each standard solution and a solution of α-CHCA in the ratio of 50 to 50 (final test compound concentration is 5 μg/mL). One microliter of each reference sample was spotted on an indium tin oxide-coated glass slide.

### 2.5. MALDI-MSI

MALDI-MSI was performed on a MALDI-ion trap-time of flight (TOF) mass spectrometer (iMScope, Shimadzu, Kyoto, Japan) [8,10]. Imaging data were obtained using Imaging MS Solution (ver. 1.20; Shimadzu) and then processed using Biomap software (version 3.8.0.4; Novartis, Basel, Switzerland) [8,10].

### 2.6. Analytical conditions

The prepared samples were analyzed in quadruplicate. First, a pulsed laser beam was used to irradiate 100 spots (as grid of 10 × 10 pixels, at a pitch of 80 μm) per sample. Subsequently, this set was shifted by a half pitch in the direction of the X-axis, the Y-axis, or both the X- and Y-axes, and irradiation with the pulsed laser beam was repeated. Data for the selection of optimal conditions were collected with total ion monitoring, and data for the LOD were collected with product ion monitoring. The optimal conditions of the iMScope are described in ESM Tab 3. Other acquisition parameters, including polarity (positive), shot per spot (100), and laser frequency (1 kHz), were held constant. The concentration was determined as the LOD when the data met the following conditions.

1. The product ion for quantification of the test compound was detected at more than 2 spots per set.
2. More than half of the four sets satisfied the above condition.

### 2.7. Calculation of coefficients of variation (CV)

The average intensity/set was calculated from the results of the intensity of 100 spots. The average intensity/sample was calculated from the results of the quadruplicate analyses (the results of 4 average intensity/set). Intra-sample CVs were calculated from the results of the average intensity/set; inter-sample CVs were calculated from the results of the average intensity/sample.

### 2.8. Statistical analysis

Spearman's correlation test was conducted using R version 3.5.2 [19]. A p-value $< 0.05$ was considered as being statistically significant. Data are presented as mean ± SD unless otherwise indicated.

## 3. Results

### 3.1. The effect of the addition of gelatin solution

A schematic of the experimental design is shown in Fig. 1. The samples that contained 1 and 2 ng/mg erlotinib were prepared in liver homogenate or liver homogenate supplemented with the gelatin solution. Then, the intensities of each sample were analyzed after treatment using α-CHCA as a matrix. The data were obtained from three separate samples (separate sections). Intra- and inter-sample CVs of values for the 1-ng/mg sample with added gelatin were 6.5–21.1% and 24.7%, respectively, while those of 1-ng/mg sample without additive were 29.8–55.5% and 46.3%, respectively. The intra- and inter-sample CVs of the 2-ng/mg sample with added gelatin were 8.7–25.5% and 18.9%, respectively, while those of the additive-free sample were 10.9–33.8% and 25.8%, respectively. Thus, at both concentrations of erlotinib, the CVs of liver homogenate with added gelatin solution were smaller than those of additive-free liver homogenate.

### 3.2. Selection of optimal conditions for detecting test compounds

We mainly investigated molecular targeted drugs, including the 12 agents listed in Table 1. MS imaging is suitable for an analysis of the heterogeneous tissues such as tumors because MS imaging has an advantage that the information on the spatial distribution of the administered drug and its metabolites in tissues are understood. Accordingly, in this study we investigated anticancer agent, especially molecular targeted drug that is one of major targets in the development of anticancer agent, those agents were selected as representative examples of molecular targeted drug. The laser power that showed the highest intensity of test compounds was selected by investigating the average intensities of 100 spots at various laser powers. The laser power was optimized for each test compound. Optimized laser powers are listed in ESM, Table S3. Liver homogenates with 50% gelatin solution were prepared for each test compound. The precursor ion intensities of different adduct ions (H, Na, K) for each test compound in liver homogenate with gelatin solution, organized by adduct ion and matrix, are shown in Fig. 2; each compound was tested at a concentration of 20 ng/mg. Two matrices, α-CHCA and DHB, were compared. The blank liver homogenate containing gelatin solution also was analyzed to confirm the selectivity of detection. For most of the test compounds, greater intensities were obtained with α-CHCA as the matrix than with DHB; similarly, for most of the test compounds, the intensities of the proton adduct ions also were greater than those of other adduct ions such as sodium and potassium. However, the signal to noise ratios using DHB were higher than that of CHCA for some compounds (erlotinib, osimeritinib, and olaparib). These results were caused that CHCA would have ionized co-existing biological components (such as salt, organic acid, lipid, sugar, protein, etc.) more efficiently than DHB. (In other words, DHB may be able to ionize these compounds more selectively than CHCA.)

The results suggested that the intensity of the precursor ion included signals from interfering components originating from liver homogenates or gelatin. The precursor ion was fragmented by collision-induced dissociation (CID) to improve selectivity, and the obtained specific fragment ions were used for detection. The collision energy was used to select the highest intensity of test compounds by investigating the average intensities of 100 spots at various collision energies. The collision energy was optimized for each test compound. Optimized collision energies, precursor ions, and specific product ions are listed in ESM, Table S3 and Fig. S1.

The LOD for each test compound was determined according to the methods described above. MS imaging at 20 ng/mg and the LOD are shown Fig. 3. The values of the LOD of each test compound were as follows: erlotinib, 0.05 ng/mg; nilotinib, 0.1 ng/mg; imatinib, 0.2 ng/mg; dasatinib, 0.5 ng/mg; gefitinib, 0.5 ng/mg; afatinib, 1 ng/mg; olaparib, 2 ng/mg; sitagliptin, 2 ng/mg; osimertinib, 5 ng/mg; and raltegravir, 5 ng/mg. The LOD of erlotinib was the lowest among the test compounds. At concentrations of 20 ng/mg, specific product ions of fluorouracil and docetaxel were not detected in liver homogenates.

### 3.3. Correlation between intensities and properties of test compounds

The correlations between the specific product ion intensities and properties (protein binding ratio, Log P, and polarizability) of test compounds were determined to better understand the properties that caused differences in the LODs among the various test compounds. The results obtained with 20-ng/mg samples were used to assess these relationships because the 20-ng/mg concentration was tested for most compounds detected in the present study. The correlations between the intensities and properties of

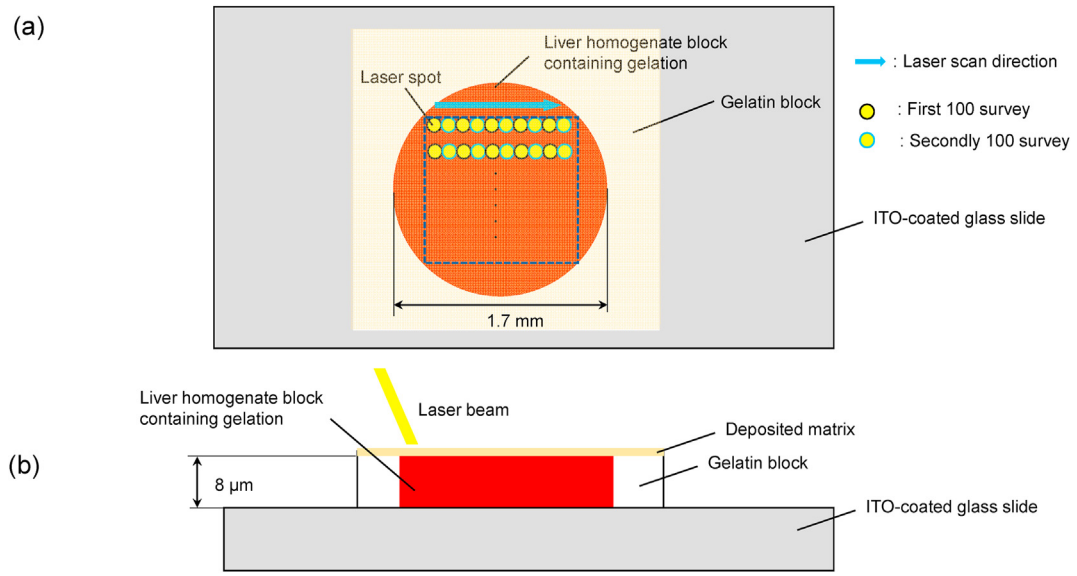


**Fig. 1.** Schematic of the experimental design. (a): top view, (b): side view A laser beam was used to irradiate liver homogenate containing gelatin solution; MS data were recorded at each X- and Y-axis position. First, a pulsed laser beam was used to irradiate 100 spots (as a grid of 10×10 pixels). Subsequently, this set was shifted by a half pitch in the direction of the X-axis, the Y-axis, or both the X- and Y-axes, and irradiation with the pulsed laser beam was repeated.

test compounds are shown in Fig. 4 and ESM Figs. S2 and S3. The values of Log P, polarizability, and protein binding ratio in plasma or serum were obtained from DrugBank or the package inserts for the respective drugs [20,21]. Osimertinib was excluded because of the low signal intensity and significant variations.

The intensity of test compounds correlated significantly with the protein binding ratio ($\rho = 0.81368$ [$p = 0.01$]), indicating that the protein binding ratio might represent a property affecting the drug ionization in tissue. It should be noted that although the protein binding ratios of test compounds correlated with both Log P and polarizability ($\rho = 0.67626$ [$p = 0.02$] and 0.68338 ($p = 0.01$), respectively), the intensities did not demonstrate significant correlations with either Log P or polarizability ($\rho = 0.60000$ [$p = 0.10$] and 0.53333 [$p = 0.15$], respectively).

We analyzed reference samples (pure compound) to investigate the protein binding affecting tissue's the drug ionization. The intensity of pure test compounds also correlated with the protein binding ratio ($\rho$= 0.81368[$p = 0.01$]).

## 4. Discussion

The aims of this study were to generate a standardized procedure for developing a MALDI-MSI assay and to explore key properties of target compounds that affect the intensities of MALDI-MSI. We developed a procedure for determining operating parameters by using an in-tissue approach [16] using liver homogenate; the procedure was independent of the specific target compound. Thus, the procedure proposed in this study should be feasible as a standard assay protocol in MALDI-MSI. Furthermore, we investigated the relationship between the intensities of target compounds (as obtained with our method) and other properties (Log P, polarizability, and protein binding ratio). Our analysis revealed that the intensity showed a correlation with the protein binding ratio, but did not correlate with either Log P or polarizability. The results suggested that the protein binding ratio should play an important role in estimating the sensitivity of a test compound in biological specimens.

The in-tissue approach is the only way to evaluate both extraction and ionization every laser shots, because a mimetic tissue closely matches the properties of the test compound present in the real sample [16,17,22]. We used a liver homogenate as a mimetic tissue because the liver is the largest organ in the body and it is easy to prepare a homogenate of this organ [17,22–24]. However, additive-free tissue (liver) homogenate shows very high viscosity. Accordingly, we adopted the liver homogenate diluted with gelatin solution as a blank sample because gelatin is a biological protein

**Table 1**
The testing compounds and those properties.

| Name | Efficacy | Molecular weight (Average) | Chemical formula | Theoretical *m/z* | | | Protein binding (%) | Log P | Polarizability |
|---|---|---|---|---|---|---|---|---|---|
| | | | | $[M+H]^+$ | $[M+Na]^+$ | $[M+K]^+$ | | | |
| Afatinib | Tyrosine kinase inhibitor | 485.9380 | $C_{24}H_{25}ClFN_5O_3$ | 486.1703 | 508.1522 | 524.1262 | 95 | 3.77 | 50.07 |
| Dasatinib | Tyrosine kinase inhibitor | 488.0060 | $C_{22}H_{26}ClN_7O_2S$ | 488.1630 | 510.1449 | 526.1189 | 96 | 2.77 | 51.58 |
| Docetaxel | Tubulin depolymerization inhibitor | 807.8792 | $C_{43}H_{53}NO_{14}$ | 808.3539 | 830.3358 | 846.3098 | 94 | 4.1 | 82.06 |
| Erlotinib | Tyrosine kinase inhibitor | 393.4357 | $C_{22}H_{23}N_3O_4$ | 394.1761 | 416.1581 | 432.1320 | 95 | 3.13 | 43.48 |
| Fluorouracil | Antimetabolites | 130.0772 | $C_4H_3FN_2O_2$ | 131.0251 | 153.0071 | 168.9810 | 8.9 | −0.58 | 9.46 |
| Gefitinib | Tyrosine kinase inhibitor | 446.9020 | $C_{22}H_{24}ClFN_4O_3$ | 447.1594 | 469.1413 | 485.1153 | 90 | 4.02 | 46.11 |
| Imatinib | Tyrosine kinase inhibitor | 493.6027 | $C_{29}H_{31}N_7O$ | 494.2663 | 516.2482 | 532.2222 | 95 | 3.47 | 55.54 |
| Nilotinib | Tyrosine kinase inhibitor | 529.5158 | $C_{28}H_{22}F_3N_7O$ | 530.1911 | 552.1730 | 568.1470 | 98 | 4.51 | 52.35 |
| Olaparib | Tyrosine kinase inhibitor | 434.4628 | $C_{24}H_{23}FN_4O_3$ | 435.1827 | 457.1646 | 473.1386 | 82 | 2.68 | 44.03 |
| Osimertinib | Tyrosine kinase inhibitor | 499.6190 | $C_{28}H_{33}N_7O_2$ | 500.2769 | 522.2588 | 538.2327 | 95 | 4.47 | 56.84 |
| Raltegravir | Antiviral | 444.4163 | $C_{20}H_{21}FN_6O_5$ | 445.1630 | 467.1450 | 483.1189 | 83 | −0.39 | 42.47 |
| Sitagliptin | Hypoglycemic agent | 407.3136 | $C_{16}H_{15}F_6N_5O$ | 408.1254 | 430.1073 | 446.0812 | 38 | 1.95 | 32.66 |

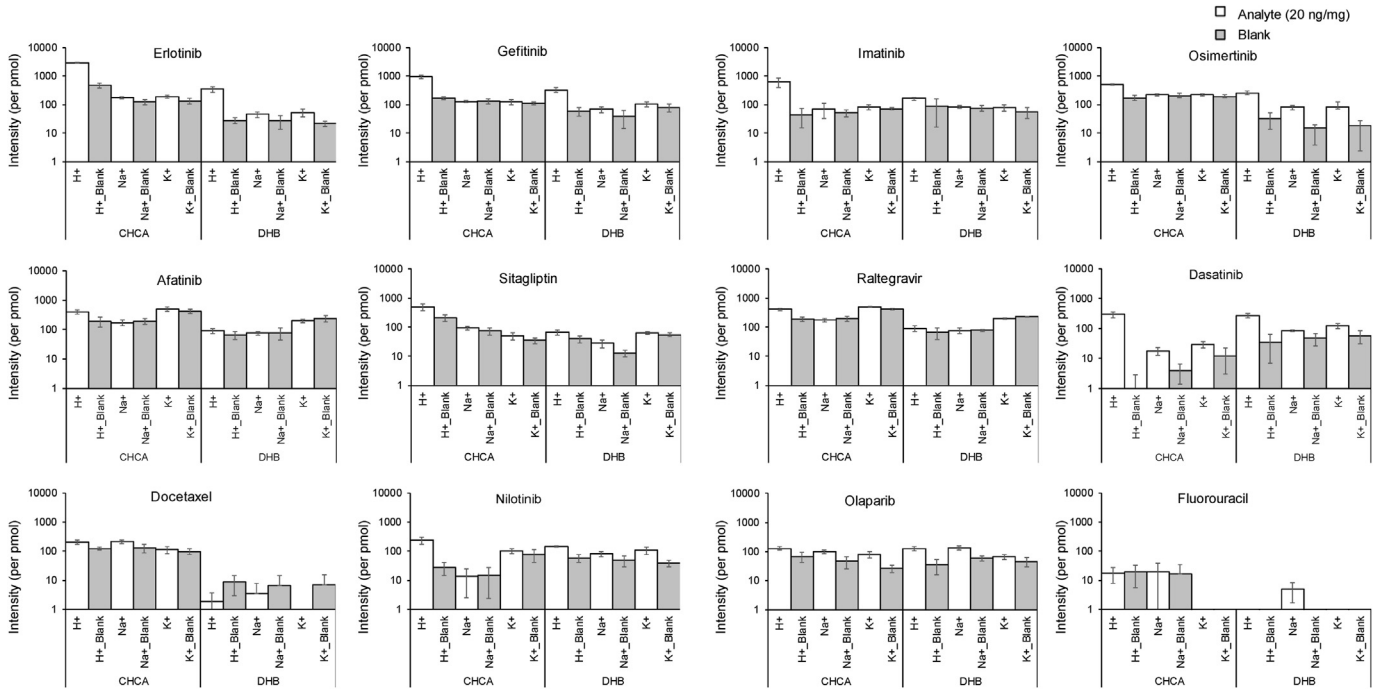


**Fig. 2.** Intensity of each adduct ion of blank and analyte samples. The signals shown in blank samples are interfering signals originating from liver homogenates or gelatin because of poor mass resolution power. Thus, signals of test compounds sample also include interfering signals. Intensities were converted to units of per pmol. Data are presented as mean ± SD (n=4).

obtained from collagen and often is used as an embedding medium and surrogate material in MALDI-MSI [25–28]. The present study indicated that the tissue homogenate diluted with a gelatin solution is an effective matrix for improving intensity variation. We consider that the low intensity variation is the most important at MALDI-IMS method development. We infer that this advantage (compared to unsupplemented liver homogenate) is caused by improved homogeneity, miscibility, and tissue homogenate handling following dilution with the gelatin solution. This is a major advantage because normalizing analyte ion intensity using reference compounds is difficult to improve the variation of the intensity due to the poor homogeneity, miscibility, and tissue homogenate handling. Moreover, using the study procedure proposed here, it is possible to examine multiple concentrations in one section because the sample blocks were prepared by injecting tissue homogenates diluted with gelatin solution into holes in solidified gelatin. In the context of method development, it is advantageous to be able to select operating parameters based on the results from one sample. In addition, we were able to select operating parameters by confirming reproducibility because the present study procedure enabled analysis in quadruplicate.

In our experience, it is thought that compounds that contain ionic functional moieties with high hydrophilicity have a tendency to be ionized efficiently, yielding a high sensitivity. In the present study, however, higher sensitivities were obtained for the compounds with higher protein binding ratios; such compounds typically show higher hydrophobicities [29]. Hydrophobicity typically is evaluated by polarizability and Log P. We also confirmed the correlation between protein binding ratio and the parameters of polarizability and Log P in this study. The intensities of ions correlated with protein binding ratio; however, these did not relate to polarizability or Log P.

Thus, these results suggest that the polar character of the compound does not directly influence the sensitivity of MALDI-MSI. Instead, the protein binding ratio is a crucial factor. When the pure compound is analyzed, only the compound will receive the protons generated from the matrix. On the other hand, when a biological sample is analyzed, test compounds and other components are simultaneously ionized because biological samples include many components (such as salt, organic acid, lipid, protein, etc.). Thus, those compounds compete for protons (this is called the “matrix effect”). In this study, the protein binding ratio showed the correlation with the intensity of pure test compound and that of the test compound in liver homogenate diluted with gelatin solution. We guessed that it would not be critical for MALDI's ionization efficiency whether the compound is binding to the protein, the protein binding ratio as physical property would be a key.

The general principle of MALDI revolves around the rapid photovolatilization of a sample embedded in a UV-absorbing matrix [30]. The analytes mixed with a matrix solution form a crystal. The irradiation of this mixture by a laser induces the ionization of the matrix, followed by desorption and then the transfer of protons from the photo-excited matrix to the analyte to form a protonated molecule. Nishikaze et al. [31] have reported that the ionization yield Ji can be expressed as

$$\mathrm{Ji} = I \times \mathrm{Jv}$$

(*I*: ionization efficiency, Jv: the rate of desorption or vaporization of neutral molecules)

They have reported that *I* can be related to thermochemical quantities such as proton affinity (protonated form), Jv can be related to aromaticity in MALDI [31,32]. On the other hand, the driving forces for protein binding come from intermolecular interaction such as hydrophobic interactions, electrostatic interactions, hydrogen bonds, and van der Waals forces. Proton affinity and aromaticity are closely related to hydrogen bonding and

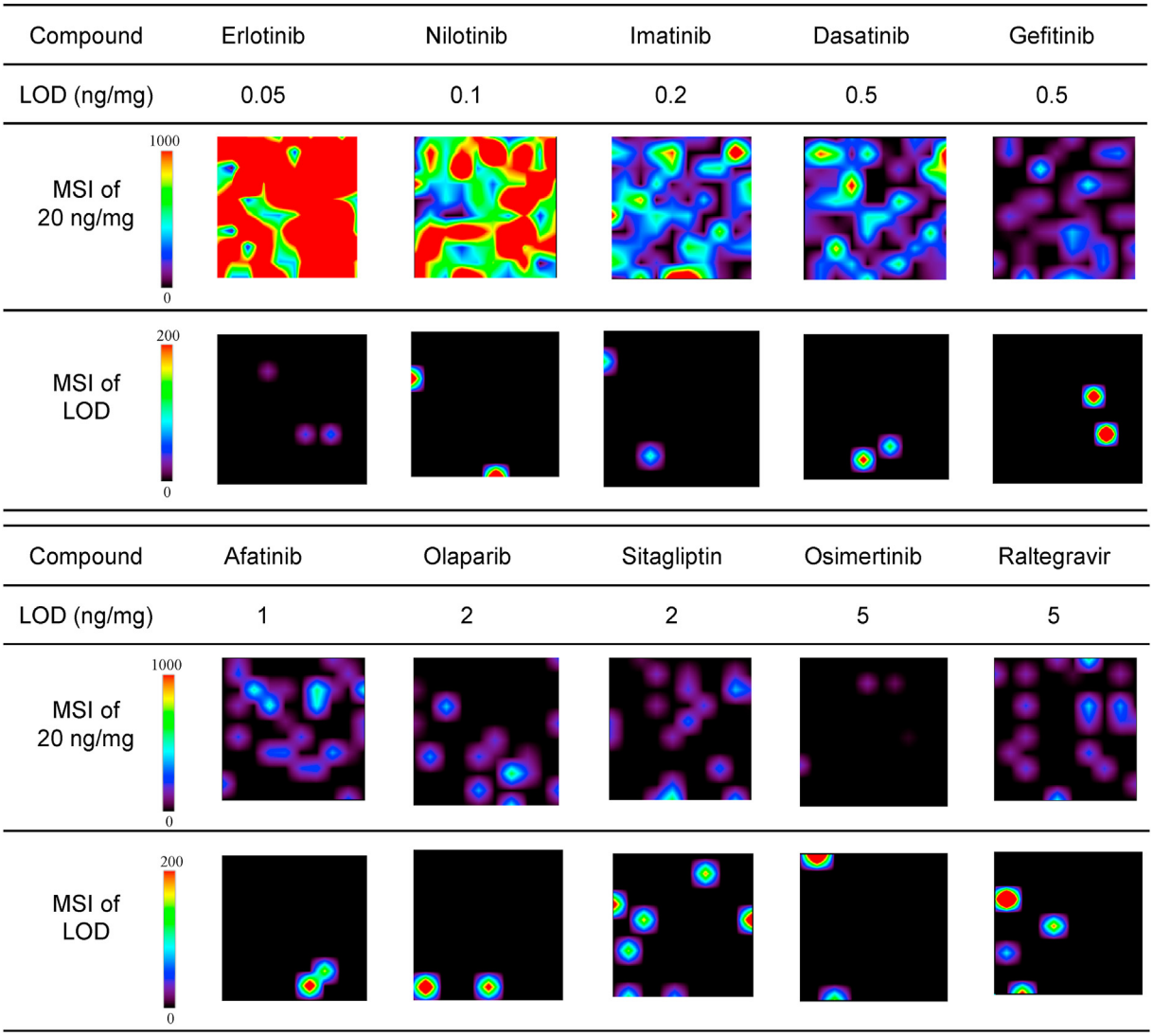


**Fig. 3.** MALDI-MS imaging at 20 ng/mg and LOD in liver homogenate containing gelatin solution LOD: Limit of detection, Mass tolerance is ± 0.02 Da, Twenty nanograms per milligram is equivalent to 20 μg/mL when the density of the liver homogenate diluted with gelatin solution is 1 g/mL.

hydrophobic interactions. Therefore, we estimated that the protein binding rate correlated with the ion intensity.

We could not detect a specific product ion for docetaxel, and could hardly detect a specific product ion for osimertinib at 20 ng/mg, suggesting that the theory described above is not applicable to those compounds. Because MALDI-MSI includes a highly complex ionization process, it is difficult to estimate the intensities of all compounds with only one parameter such as protein binding ratio. We did not include fluorouracil in the theory described above since its specific product ion was not detected at 20 ng/mg; however, the low intensity of fluorouracil may be caused by low protein binding.

The present study suggested that liver homogenate diluted with gelatin solution is a useful matrix for the development of analytical methods for MALDI-MSI. The present study also indicated the possibility that the protein binding ratio plays an important role in estimating the sensitivity of a target compound in biological specimens. Our results in this study were investigated mostly using anticancer agents, however, our results would be applicable to other character (physicochemical property and pharmacological action etc) drugs. Furthermore, our results could not be applied successfully to all compounds, suggesting that parameters other than the protein binding ratio should be investigated. In this work, we did not conduct normalization and correction with a reference compound; the use of such a reference compound, preferably a labeled version of the target analyte would be an obvious next step [33,34]. The utility of a reference compound to reduce the intensity variability and increase data quality in our protocols would need to be evaluated. Additionally, the investigation of quantification would be essential [35,36]. The difference of matrix effect between the calibration sample and test sample will lead to overestimation or underestimation of concentrations, when calibration samples are not the same with test samples (for example, calibration samples are prepared from liver homogenate diluted with gelatin solution, test samples are tumor). However, there are many issues to be resolve for quantification by MALDI-MSI. Although, the normalization analyte ion intensity using reference compounds is one of the solutions the normalization analyte ion intensity dose not resolve all issues. (For example, the stability of prepared sample, the determination of LLOQ, the preparation method of QC sample, and differences in the size of the ROI (region of interest) between calibrated and real samples etc. Therefore, we did not investigate to quantify in this study.) Quantification by MALDI-MSI

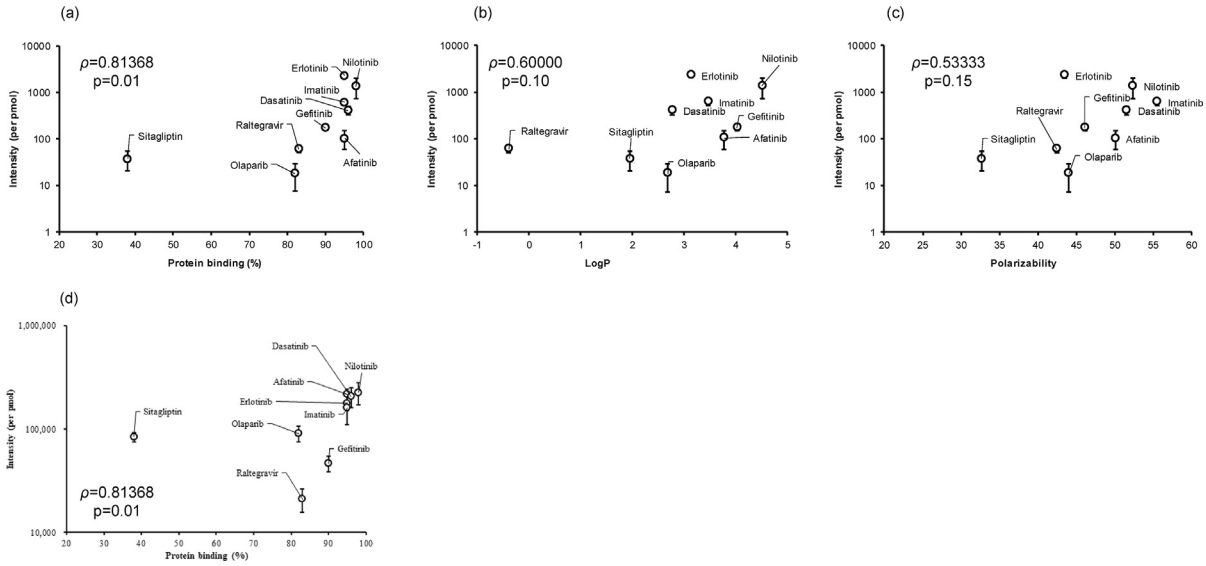


**Fig. 4.** Correlation analysis between intensity and test compound properties.
(a) Correlation between intensity and protein binding. (b) Correlation between intensity and Log P. (c) Correlation between intensity and polarizability. (d) Correlation between intensity and protein binding. *ρ (pho)*: Spearman's rank correlation coefficient. p: p-value. Intensities were converted to units of per pmol. The protein binding ratio in plasma or serum was referred to as the database (DrugBank [Wishart et al., 2015] or the package inserts for the respective drugs [PMDA]).Data are presented as mean ± SD (n= 4).Intensities (a, b, c) are in liver homogenate containing gelatin solution. Intensities (d) are from pure testing compounds.

would be a major challenge. The approaches of the present study should remain valid for other types of mass analyzers such as quadrupole-TOF [37], Kingdontrap [38], fourier transform ion cyclotron resonance mass spectrometry (FT-ICR) [39] and, so on. A procedure for standardization of method development by MALDI-MSI assay protocol would contribute to the acquisition of reproducible data. The insight that protein binding ratio correlates with the sensitivity of the target compound would allow the sensitivity of the target compound in biological samples to be estimated. It is currently difficult to obtain highly reproducible, highly selective, highly specific, and quantitative data on the distribution of drugs or biomarkers in tissue; however the investigations of normalization and correction with a reference compound and quantification would contribute to obtaining such data by MALDI-MSI. Such data are essential to provide new applications and insights into molecular processes, facilitating the efficient evaluation of drugs in preclinical studies to develop new pharmaceutical products.

In conclusion, we presented a procedure for standardization of method development by MALDI-MSI assay protocol and indicated the possibility that the protein binding ratio indicates the sensitivities of target compounds. It is hoped that the present approach will contribute to further progress in the application of MALDI-MSI techniques and the ability to develop suitable assay protocols.

## Authors' contributions

Y·H., M.O., and A.H. conceived and designed the experiments. Y.H. and M.O. conducted mass spectrometry imaging, and data analysis. Y.H. wrote the main manuscript with feedback from all authors. M.O., S.R., S·Y., and A.H. contributed to the editing of the manuscript.

## Funding

Not applicable.

## Declaration of competing interest

Y.H. is an employee of CMIC Pharma Science Co., Ltd.

A.H. has received grant support from CMIC Pharma Science Co., Ltd. The other authors declare no potential conflict of interest.

## Acknowledgements

We thank Drs. N. Suzuki, E. Takahara, N. Danno and F. Nakagawa for their helpful advice.

## Appendix A. Supplementary data

Supplementary data to this article can be found online at https://doi.org/10.1016/j.dmpk.2021.100385.

## References

[1] Korfmacher WA. Foundation review: principles and applications of LC-MS in new drug discovery. Drug Discov Today 2005;10:1357–67. https://doi.org/10.1016/S1359-6446(05)03620-2.
[2] Henion J, Brewer E, Rule G. Peer reviewed: sample preparation for LC/MS/MS: analyzing biological and environmental samples. Anal Chem 1998;70:650A–6A. https://doi.org/10.1021/ac981991q.
[3] Sun N, Walch A. Qualitative and quantitative mass spectrometry imaging of drugs and metabolites in tissue at therapeutic levels. Histochem Cell Biol 2013;140:93–104. https://doi.org/10.1007/s00418-013-1127-4.
[4] Römpp A, Both JP, Brunelle A, Heeren RMA, Laprévote O, Prideaux B, et al. Mass spectrometry imaging of biological tissue: an approach for multicenter studies. Anal Bioanal Chem 2015;407:2329–35. https://doi.org/10.1007/s00216-014-8410-7.
[5] Castellino S, Groseclose MR, Wagner D. MALDI imaging mass spectrometry: bridging biology and chemistry in drug development. Bioanalysis 2011;3:2427–41. https://doi.org/10.4155/bio.11.232.
[6] Nishimura M, Hayashi M, Mizutani Y, Takenaka K, Imamura Y, Chayahara N, et al. Distribution of erlotinib in rash and normal skin in cancer patients receiving erlotinib visualized by matrix assisted laser desorption/ionization mass spectrometry imaging. Oncotarget 2018;9:18540–7. https://doi.org/10.18632/oncotarget.24928.
[7] Nishidate M, Yamamoto K, Masuda C, Aikawa H, Hayashi M, Kawanishi T, et al. MALDI mass spectrometry imaging of erlotinib administered in combination with bevacizumab in xenograft mice bearing B901L, EGFR-mutated NSCLC cells. Sci Rep 2017;7. https://doi.org/10.1038/s41598-017-17211-6.

[8] Ryu S, Hayashi M, Aikawa H, Okamoto I, Fujiwara Y, Hamada A. Heterogeneous distribution of alectinib in neuroblastoma xenografts revealed by matrix-assisted laser desorption ionization mass spectrometry imaging: a pilot study. Br J Pharmacol 2018;175:29–37. https://doi.org/10.1111/bph.14067.
[9] Tsubata Y, Hayashi M, Tanino R, Aikawa H, Ohuchi M, Tamura K, et al. Evaluation of the heterogeneous tissue distribution of erlotinib in lung cancer using matrix-assisted laser desorption ionization mass spectrometry imaging. Sci Rep 2017;7:12622. https://doi.org/10.1038/s41598-017-13025-8.
[10] Aikawa H, Hayashi M, Ryu S, Yamashita M, Ohtsuka N, Nishidate M, et al. Visualizing spatial distribution of alectinib in murine brain using quantitative mass spectrometry imaging. Sci Rep 2016;6:1–9. https://doi.org/10.1038/srep23749.
[11] Nilsson A, Goodwin RJA, Shariatgorji M, Vallianatou T, Webborn PJH, Andrén PE. Mass spectrometry imaging in drug development. Anal Chem 2015;87:1437–55. https://doi.org/10.1021/ac504734s.
[12] Hsieh Y, Chen J, Korfmacher WA. Mapping pharmaceuticals in tissues using MALDI imaging mass spectrometry. J Pharmacol Toxicol Methods 2007;55:193–200. https://doi.org/10.1016/j.vascn.2006.06.004.
[13] Caprioli RM, Farmer TB, Gile J. Molecular imaging of biological samples: localization of peptides and proteins using MALDI-TOF MS. Anal Chem 1997;69:4751–60. https://doi.org/10.1021/ac970888i.
[14] Karas M, Krüger R. Ion formation in MALDI: the cluster ionization mechanism. Chem Rev 2003;103:427–40. https://doi.org/10.1021/cr010376a.
[15] Marvin LF, Roberts MA, Fay LB. Matrix-assisted laser desorption/ionization time-of-flight mass spectrometry in clinical chemistry. Clin Chim Acta 2003;337:11–21. https://doi.org/10.1016/j.cccn.2003.08.008.
[16] Nishidate M, Hayashi M, Aikawa H, Tanaka K, Nakada N, Miura S, et al. Applications of MALDI mass spectrometry imaging for pharmacokinetic studies during drug development. Drug Metabol Pharmacokinet 2019;34:209–16. https://doi.org/10.1016/j.dmpk.2019.04.006.
[17] Groseclose MR, Castellino S. A mimetic tissue model for the quantification of drug distributions by MALDI imaging mass spectrometry. Anal Chem 2013;85:10099–106. https://doi.org/10.1021/ac400892z.
[18] Schulz S, Becker M, Groseclose MR, Schadt S, Hopf C. Advanced MALDI mass spectrometry imaging in pharmaceutical research and drug development. Curr Opin Biotechnol 2019;55:51–9. https://doi.org/10.1016/j.copbio.2018.08.003.
[19] R Development Core Team R. A language and environment for statistical computing. R Found Stat Comput Vienna Austria; 2011. https://doi.org/10.1038/sj.hdy.6800737 {ISBN} 3-900051-07-0.
[20] Wishart DS, Feunang YD, Guo AC, Lo EJ, Marcu A, Grant JR, et al. DrugBank 5.0: a major update to the DrugBank database for 2018. Nucleic Acids Res 2018;46:D1074–82. https://doi.org/10.1093/nar/gkx1037.
[21] Pharmaceuticals, Medical Devices Agency TJ. Instructions for package inserts of prescription drugs n.d. http://www.info.pmda.go.jp/psearch/html/menu_tenpu_base.html. [Accessed 23 January 2019].
[22] Barry J, Barry JA, Groseclose MR, Fraser DD, Castellino S. Revised preparation of a mimetic tissue model for quantitative imaging mass spectrometry. Protoc Exch 2018;1–20. https://doi.org/10.1038/protex.2018.104.
[23] Jadoul L, Longuespée R, Noël A, De Pauw E, De E, Berlin S-V. A spiked tissue-based approach for quantification of phosphatidylcholines in brain section by MALDI mass spectrometry imaging. Anal Bioanal Chem 2015;407:2095–106. https://doi.org/10.1007/s00216-014-8232-7.
[24] Takai N, Tanaka Y, Saji H. Quantiication of small molecule drugs in biological tissue sec-tions by imaging mass spectrometry using surrogate tissue-based calibration standards. Mass Spectrom Tokyo 2014;3:25. https://doi.org/10.5702/massspectrometry.A0025.
[25] Rzagalinski I, Volmer DA. Quantification of low molecular weight compounds by MALDI imaging mass spectrometry – a tutorial review ☆. BBA - Proteins Proteomics 2017;1865:726–39. https://doi.org/10.1016/j.bbapap.2016.12.011.
[26] Swales JG, Hamm G, Clench MR, Goodwin RJA. Mass spectrometry imaging and its application in pharmaceutical research and development: a concise review. Int J Mass Spectrom 2019;437:99–112. https://doi.org/10.1016/j.ijms.2018.02.007.
[27] Sturtevant D, Lee Y-J, Chapman KD. Matrix assisted laser desorption/ionization-mass spectrometry imaging (MALDI-MSI) for direct visualization of plant metabolites in situ. Curr Opin Biotechnol 2016;37:53–60. https://doi.org/10.1016/j.copbio.2015.10.004.
[28] Nelson KA, Daniels GJ, Fournie JW, Hemmer MJ. Optimization of whole-body zebrafish sectioning methods for mass spectrometry imaging. J Biomol Tech 2013;24:119–27. https://doi.org/10.7171/jbt.13-2403-002.
[29] Ghuman J, Zunszain PA, Petitpas I, Bhattacharya AA, Otagiri M, Curry S. Structural basis of the drug-binding specificity of human serum albumin. J Mol Biol 2005;353:38–52. https://doi.org/10.1016/j.jmb.2005.07.075.
[30] Gross JH. Mass spectrometry. Cham: Springer International Publishing; 2017. https://doi.org/10.1007/978-3-319-54398-7.
[31] Nishikaze T, Takayama M. Study of factors governing negative molecular ion yields of amino acid and peptide in FAB, MALDI and ESI mass spectrometry. Int J Mass Spectrom 2007;268:47–59. https://doi.org/10.1016/j.ijms.2007.08.004.
[32] Nishikaze T, Takayama M. Cooperative effect of factors governing molecular ion yields in desorption/ionization mass spectrometry. Rapid Commun Mass Spectrom 2006;20:376–82. https://doi.org/10.1002/rcm.2316.
[33] Trede D, Kobarg JH, Oetjen J, Thiele H, Maass P, Alexandrov T. On the importance of mathematical methods for analysis of MALDI-imaging mass spectrometry data. J Integr Bioinforma 2012;9:189. https://doi.org/10.1515/jib-2012-189.
[34] Deininger SO, Cornett DS, Paape R, Becker M, Pineau C, Rauser S, et al. Normalization in MALDI-TOF imaging datasets of proteins: practical considerations. Anal Bioanal Chem 2011;401:167–81. https://doi.org/10.1007/s00216-011-4929-z.
[35] Hamm G, Bonnel D, Legouffe R, Pamelard F, Delbos JM, Bouzom F, et al. Quantitative mass spectrometry imaging of propranolol and olanzapine using tissue extinction calculation as normalization factor. J Proteomics 2012;75:4952–61. https://doi.org/10.1016/j.jprot.2012.07.035.
[36] Porta T, Lesur A, Varesio E, Hopfgartner G. Quantification in MALDI-MS imaging: what can we learn from MALDI-selected reaction monitoring and what can we expect for imaging? Anal Bioanal Chem 2015;407:2177–87. https://doi.org/10.1007/s00216-014-8315-5.
[37] Trim PJ, Djidja MC, Atkinson SJ, Oakes K, Cole LM, Anderson DMG, et al. Introduction of a 20 kHz Nd:YVO4 laser into a hybrid quadrupole time-of-flight mass spectrometer for MALDI-MS imaging. Anal Bioanal Chem 2010;397:3409–19. https://doi.org/10.1007/s00216-010-3874-6.
[38] Perry RH, Cooks RG, Noll RJ. Orbitrap mass spectrometry: instrumentation, ion motion and applications. Mass Spectrom Rev 2008;27:661–99. https://doi.org/10.1002/mas.20186.
[39] Ferey J, Marguet F, Laquerrière A, Marret S, Schmitz-Afonso I, Bekri S, et al. A new optimization strategy for MALDI FTICR MS tissue analysis for untargeted metabolomics using experimental design and data modeling. Anal Bioanal Chem 2019;411:3891–903. https://doi.org/10.1007/s00216-019-01863-6.

**Drug Metabolism and Pharmacokinetics**

**Supplementary Material**

# A procedure for method development and protein binding ratio as the indicator of sensitivity with anticancer agents on MALDI mass spectrometry imaging

Yoshiharu Hayashi, Mayu Ohuchi, Shoraku Ryu, Shigehiro Yagishita, Akinobu Hamada

**Tab. S1** Matrix deposit conditions (SMALDIprep)

Applied compounds were afatinib, dasatinib, erlotinib, gefitinib, imatinib, nilotinib, olaparib, osimertinib and raltegravir.

| **Parameters** | **Setting** |
|---|---|
| Gas | Nitrogen |
| Gas flow rate | 5 L/min |
| Matrix flow rate | 5 µL/min |
| Rotation speed | 350 rpm |
| Sprayer Hight | 56.3 mm |
| Time for spraying | α-CHCA : 22min<br>DHB : 30min |

**Tab. S2** Matrix deposit conditions (hand spray)

Applied compounds were docetaxel, fluorouracil and sitagliptin.

| **Parameters** | **Setting** |
|---|---|
| Gas | Nitrogen |
| Nozzle size | 0.2 mm |

**Tab. S3** MALDI-MS analytical conditions of the testing compounds

| Compound | Precursor ion | Specific product ion | Laser Power | Collison energy (%) |
|---|---|---|---|---|
| Afatinib | 486.17 | 371.07 | 49 | 65 |
| Dasatinib | 488.16 | 401.10 | 41 | 70 |
| Docetaxel | 830.34 | 549.20 | 52 | 47 |
| Erlotinib | 394.17 | 336.14 | 47 | 65 |
| Fluorouracil | 131.03 | 103.05 | 60 | 55 |
| Gefitinib | 447.16 | 128.10 | 49 | 65 |
| Imatinib | 494.26 | 394.16 | 49 | 54 |
| Nilotinib | 530.19 | 289.10 | 51 | 50 |
| Olaparib | 435.18 | 367.15 | 50 | 50 |
| Osimertinib | 500.27 | 455.20 | 47 | 55 |
| Raltegravir | 445.16 | 361.13 | 46 | 38 |
| Sitagliptin | 408.13 | 235.08 | 55 | 47 |

Afatinib (precursor ion was *m/z* 486.17)

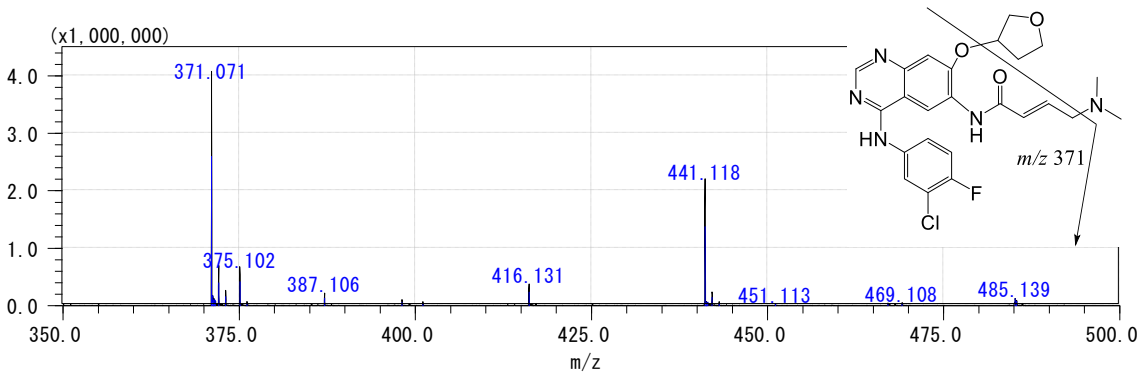


Dasatinib (precursor ion was *m/z* 488.16)

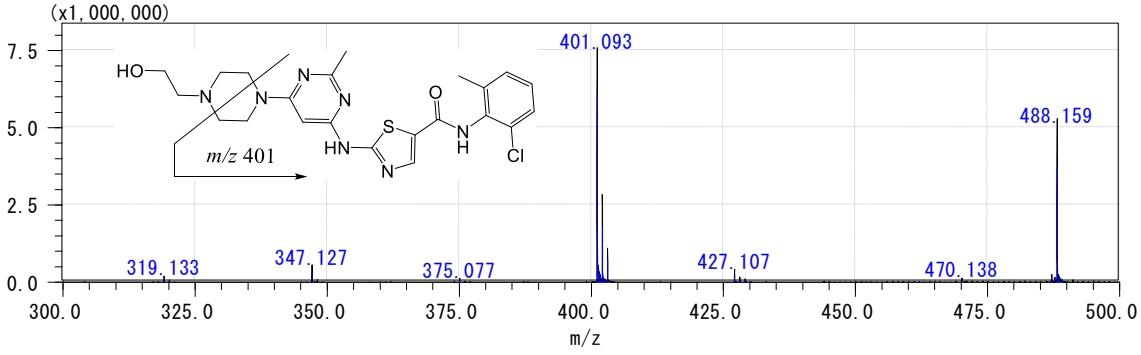


Docetaxel (precursor ion was *m/z* 830.34)

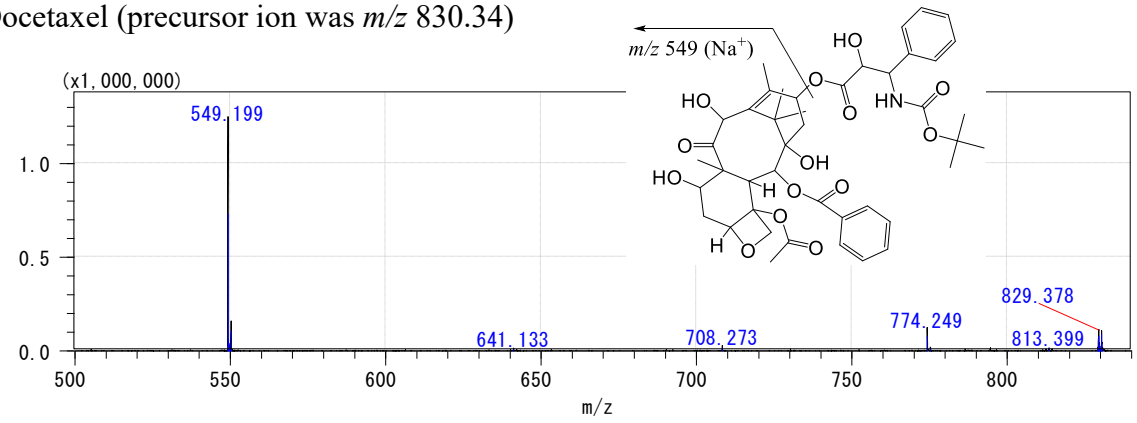


**Fig. S1** The spectra of product ion scan of target compounds by MALDI-MS

Erlotinib (precursor ion was *m/z* 394.17)

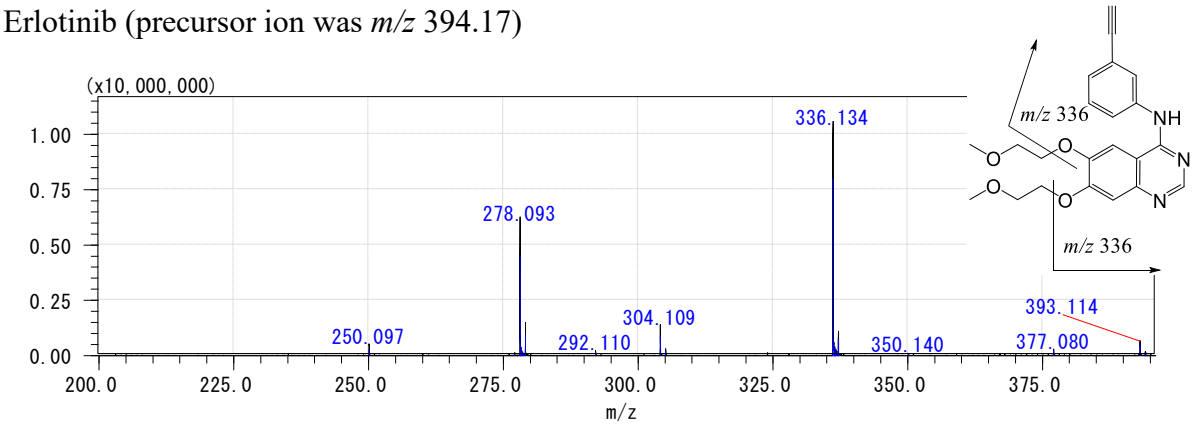


Fluorouracil (precursor ion was *m/z* 131.03)

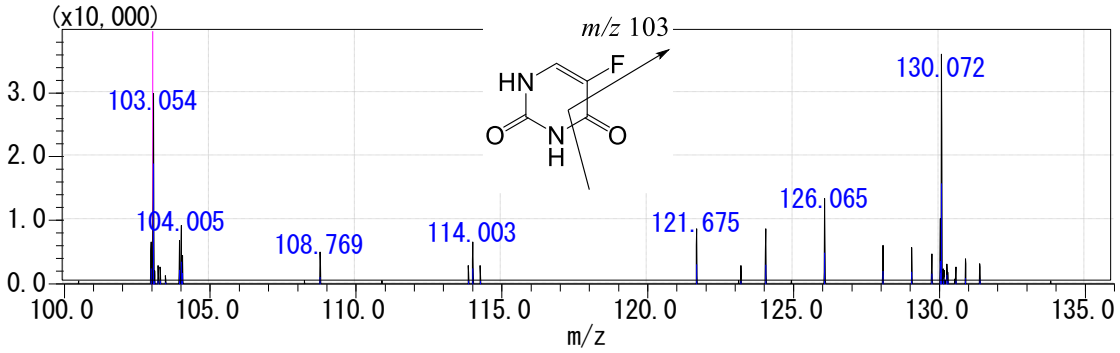


Gefitinib (precursor ion was *m/z* 447.16)

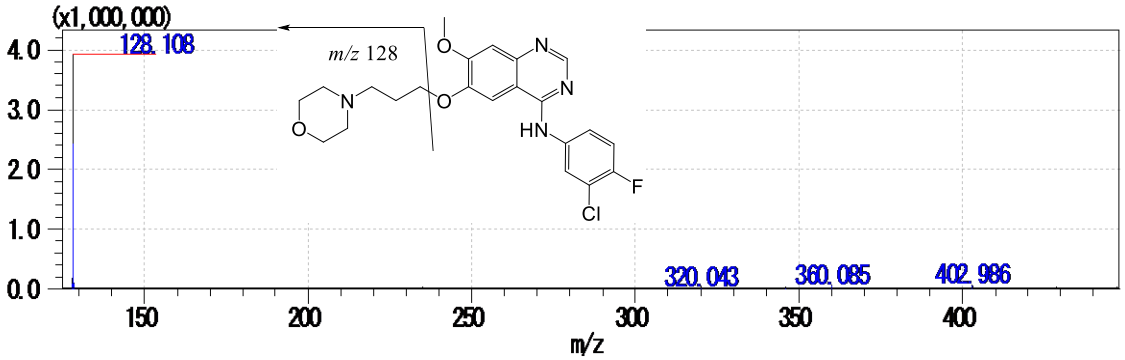


**Fig. S1** Continued

Imatinib (precursor ion was *m/z* 494.26)

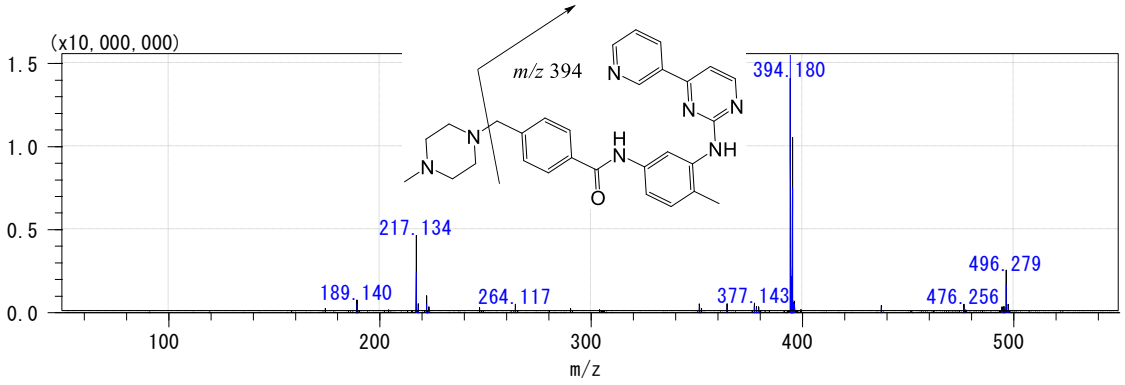


Nilotinib (precursor ion was *m/z* 530.19)

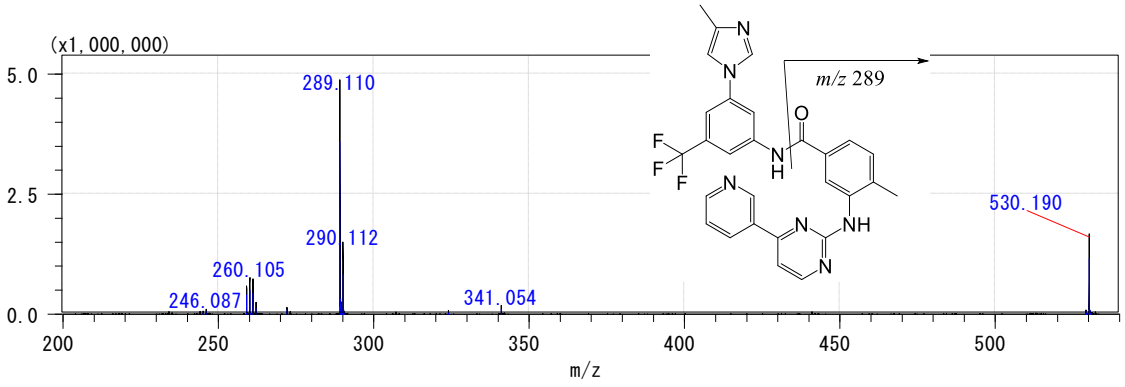


Olaparib (precursor ion was *m/z* 435.18),

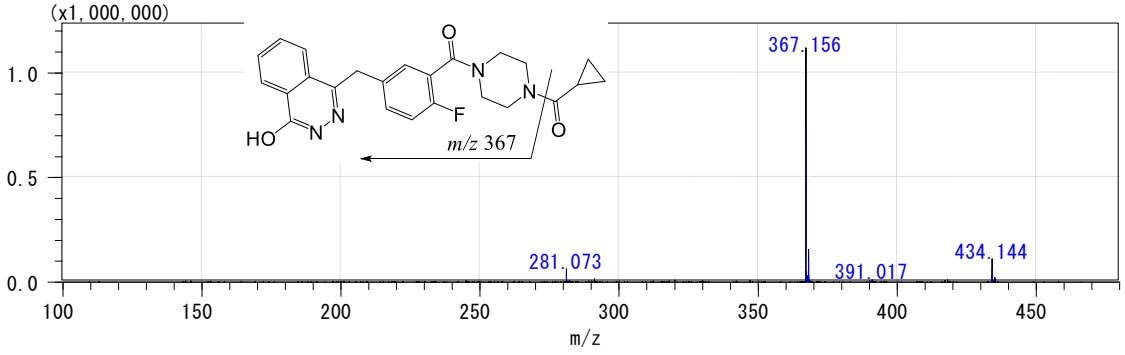


**Fig. S1** Continued

Osimertinib (precursor ion was *m/z* 500.27)

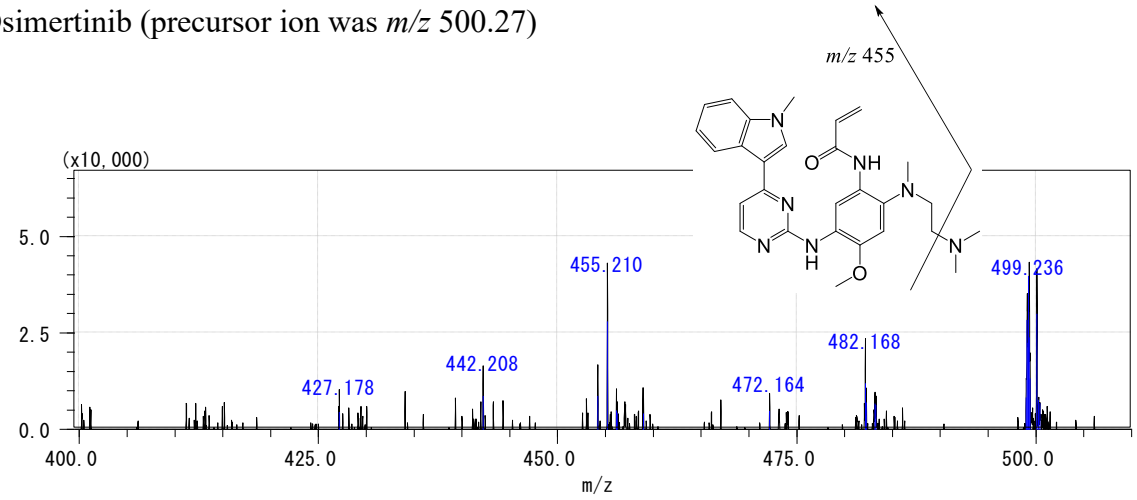


Raltegravir (precursor ion was *m/z* 445.16)

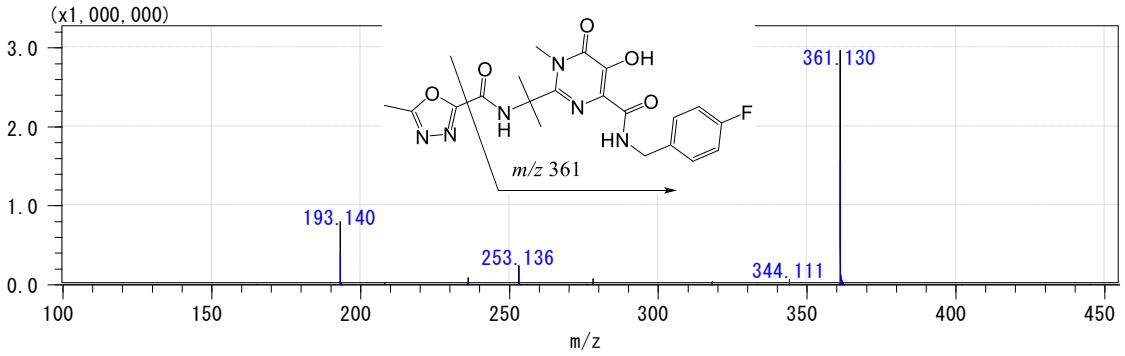


Sitagliptin (precursor ion was *m/z* 408.13)

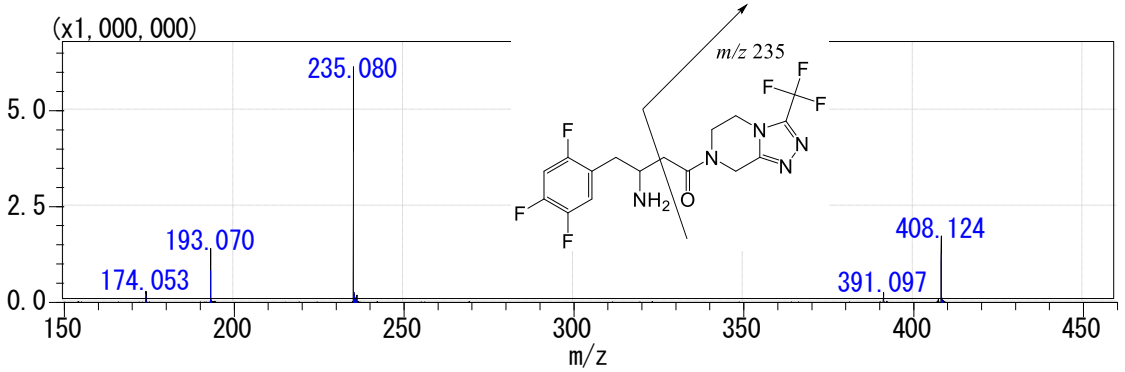


**Fig. S1** Continued

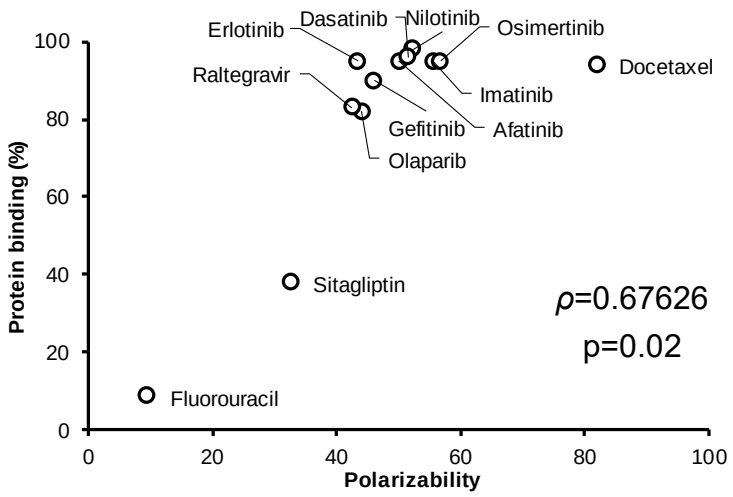


**Fig. S2** Correlation between intensity and polarizability

$\rho$ : Spearman's rank correlation coefficient.

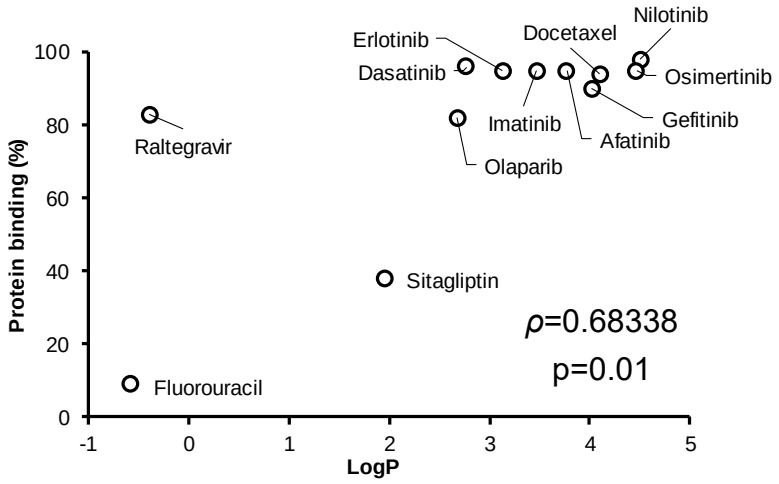


**Fig. S3** Correlation between protein binding and Log P

$\rho$ : Spearman's rank correlation coefficient.